VAR compensator to enhance the voltage profile for remote induction motor loads", to be published in Electric Power Systems Reserach Journal, 1998.

[22] Jiang, j. , and Holtz. J., "High dynamic speed sensorless AC drive with online model parameter tuning for steady-state accuracy", IEEE Trans. on Industrial Electronics, Vol. 44, No. 2, pp 240-246, April 1997.

[23] Holtz, J, "Method for speed sensorless control of ac drives", in Sensorless Control of AC Motor Drives, Rajashekara K., Kawamura. A, and Matsuse. K, Eds. Piscataway, NJ: IEEE Press, 1996.

[24] Cilia, J, Asher. G. M, Bradley. K. J, and Summer. M, "Sensorless Position detection for vector controlled induction motor drives using an asymmetric outer-section cage", IEEE Trans. on Industry Applications, Vol. 33, No. 5, pp 1162-1169, Sept/Oct 1997.

[25] Fletcher. J. E, Holliday. d, and Williams, B, W, "Non-invasive rotor position and speed sensing of asynchronous motors" in Proc. EPE Conf., Vol. 1, pp 333-337, Seville. Spain, 1995.

[26] Anderson. P.M. and Fouad. A. A. " Power system control and stability", The Iowa State University Press, USA, 1977.

[27] Kraus. P. C., " Analysis of electric machinery", Mc Graw-Hill, USA, 1986.

[28] Hiskens, I, A., and Hill. D. J, "Incorporation of SVCs into energy function method", IEEE Trans. Power system, Vol. 7, No. 1, 1992, pp 133-140.

[29] Cheng. C. H., and Hsu. Y. Y., "Damping of generator oscillation using an adaptive static var compensator", IEEE Trans. Power Systems, Vol. 7, No. 2, 1992. pp 718-795.

[30] Lee. C. C. , "Fuzzy logic in control systems: fuzzy logic controller , Part I, II", IEEE Trans. System, Man and Cybernetics, Vol. 20. 2, pp 404-435, 1990.

[31] Kosko. B. "Neural networks and fuzzy systems: A dynamic approach to machine intelligence", Printice Hall, USA, 1992.

dustry Applications, Vol. 26, No. 4, pp. 620-626, July/Aug 1990.

[3] IEEE PES Power Transmission and Distribution Ctte., Voltage Flicker and Service to Critical Loads Working Group and Ward D. J, chmn, "Power quality two different perspectives", IEEE Trans. Power Delivery, Vol. 5, No. 3, pp 1501-1513, july 1990.

[4] Hammed. A. E, "Analysis of power system stability by static var compensator", IEEE Trans. Power Systems, Vol. 1, No. 4, pp 222-227, Nov. 1986.

[5] Zhou. E. Z, "Application of static var compensators to increase power system damping", IEEE/ PES Winter Meeting, #92 WM 164-4 PWRS, New York, NY, Jan 26-30, 1992.

[6] Wong, W. k, Osborn. D. L, and McAvoy. J. L, "Application of compact static var compensators to distribution systems", IEEE Trans Power Delivery, Vol. 5, No. 2, pp 1113-1120, April 1990.

[7] Das. J. C, "Effect of momentary voltage dips on the operation of induction and synchronous motors", IEEE Trans. Industry Applications, Vol. 26. No. 4, pp 711-718, july/Aug 1990.

[8] Mulukutla. S. S, and Gulachenski. E. M, " A critical survey of considerations in maintaining process continuity during voltage dips while protecting motors with reclosing and bus-transfer practices", IEEE Trans. Power Systems, Vol. 7, No. 3, pp 1299-1305, Aug 1992.

[9] El-Sadek. M. Z, and Fetih N. H, "Starting of induction motors by static var compensators", IEE conf. Publ. No. 291, pp 444-447, 1988.

[10] El-Sadek, M. Z, "Static var compensators for reducing energy losses in large industrial loads", Journal of Electric Power System Research , Vol. 22, pp 121-133, 1991.

[11] Hammed. A. E, and El-Sadek, M. Z, "Prevention of transient voltage instabilities due to induction motor loads by static var compensators", IEEE Trans PWRS-4, No. 3, pp 1182-1190, Aug 1989.

[12] Darainkov. D., Hellendoorn. H., and Reinfrank. M. "An introduction to fuzzy control", Spring-Verlag, 1993.

[13] Hassan. M. A., Malik, O. P., and Hope , G. S. "A fuzzy logic based stabilizer for synchronous generator ", IEEE. Trans. Energy Conversion, vol. 6, No. 3, pp 407-413, 1991.

[14] El - Metwally. K. A., and Malik, O. P, "Fuzzy logic power system stabilizer", IEEE Proc. Generation, Transmission, and Distribution, Vol. 142, No. 3, pp 277-281, 1995.

[15] El-Metwally. k. A., and Malik. O. P, "Application of fuzzy logic stabilizers in multimachine power system environment", IEE Proc. Generation, Transmission, and Distribution, Vol. 143, No. 3, pp 263-260, 1996.

[16] Iisu, Y. Y., and Cheng. c. H, " A fuzzy controller for generator excitation control", IEEE Trans. System, Man, and Cybernetics, Vol. 23, No. 2, pp 532-539, 1993.

[17] Indulcar. C., S., and Raj, B, "Application of fuzzy controller to automatic generation control", Journal of Electrical Machine and Power Systems, Vol. 23 pp 209-220, 1995.

[18] Ju. P., Handschin, E., and Reyer. F. "Genetic algorithm aided controller design with application to SVC ", IEE Proc., Generation . Transmission. Distribution., Vol. 143, No. 3, pp. 258-262, 1996.

[19] Tan. O. T., Paap. G. C., and Kolluru. M. S, "Thyristor controlled voltage regulators for critical induction motor loads during voltage disturbances", IEEE. Trans. Energy Conversion, Vol. 8. No. 1, pp 100-106, March 1993.

[20] Tan, O. T, and Thohappillil, R, "Static var compensators for critical synchronous motor loads during voltage dips", IEEE Trans. PWRS-9, No. 3, pp 1517-1523, Aug 1994.

[21] Abedi, M. S. A. Taber, A. K, Sedigh, H. Seifi, "Controller design using μ synthesis for static

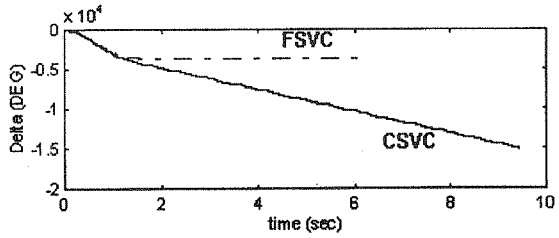

Fig. (20) Rotor angle variations of the equivalent synchronous during fault analysis test

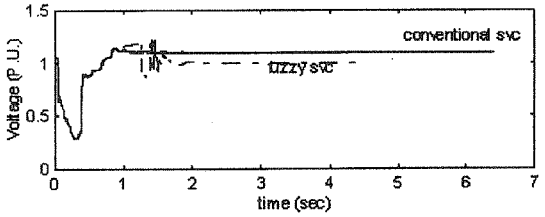

Fig (21) Voltage for the main terminal busbar (Vt) due to voltage dips in the external network

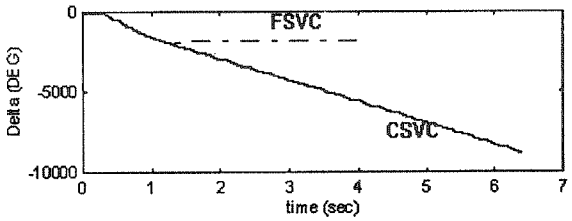

Fig . (22) Rotor angle variations of the synsnchronous machine during voltage dips test

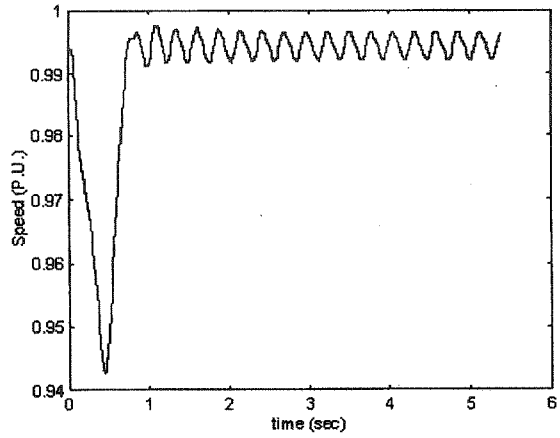

(a)

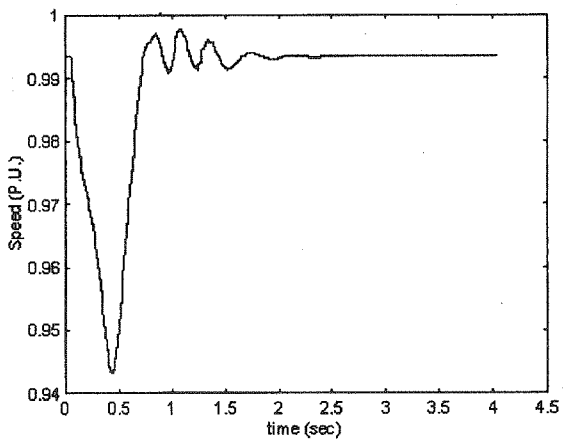

(b)

(a): CSVC , (b) : FLSVC

Fig. (23) Speed variations of the double cage motors during voltage dips test

Table (7) Parameters for each static load.

	static loads
R load (pu)	16
X load (pu)	12

References

[1] Flory. J. E, Key. T.S. etal., "The electric utility-industrial user partnership in solving power quality problems", IEEE Trans. Power Systems. Vol. 5, No. 3, pp. 878-886, Aug 1990.

[2] Wagner. V.E, and Andershak. A. A, "Power quality and factory automation". IEEE Trans. In-

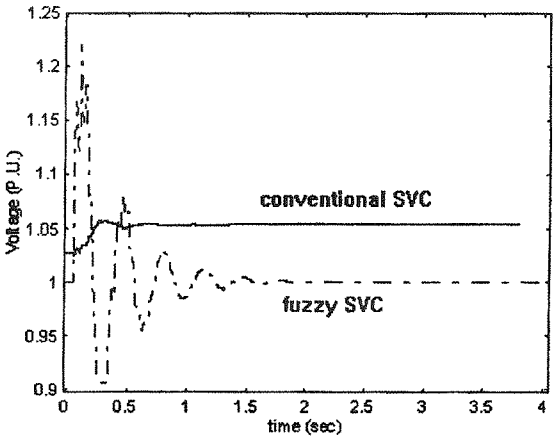

Fig. (15) Main terminal voltage (Vt) during the sudden loading period

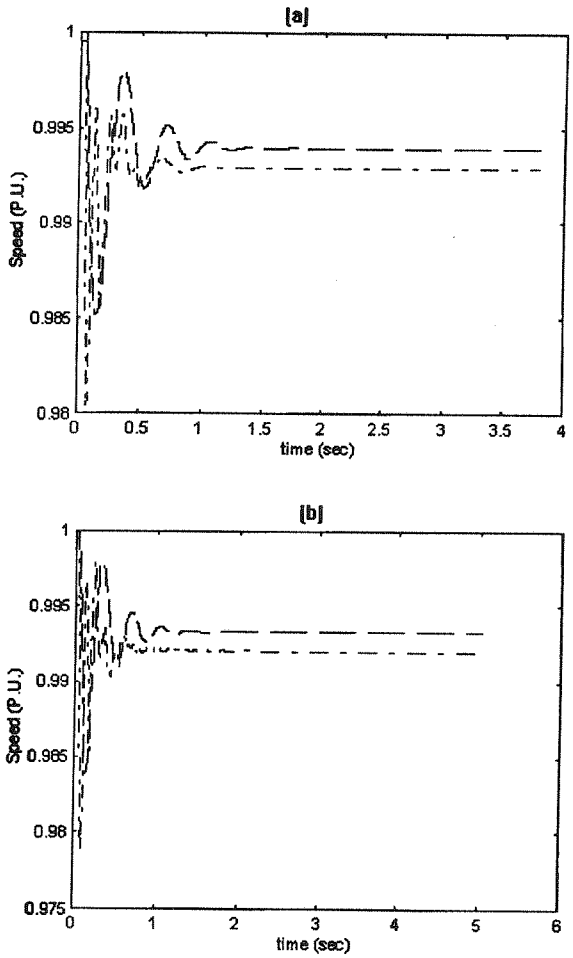

——— EDCAM , – . –. – ESCAM
(a) : CSVC, (b) : FLSVC

Fig. (16) Speed variations of equivalent single and double cage asynchronous motors during the sudden loading test

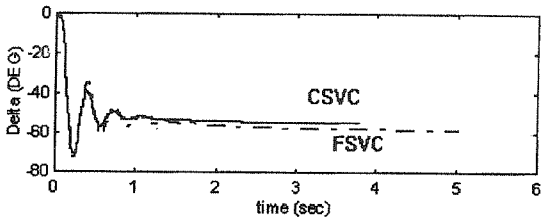

Fig. (17) Rotor angle variations of equivalent synchronous motors during the sudden loading test

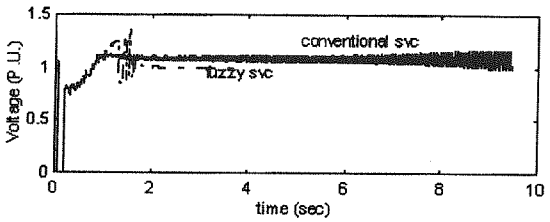

Fig. (18) Voltage variations for the main terminal busbar (vt) during fault analysis test

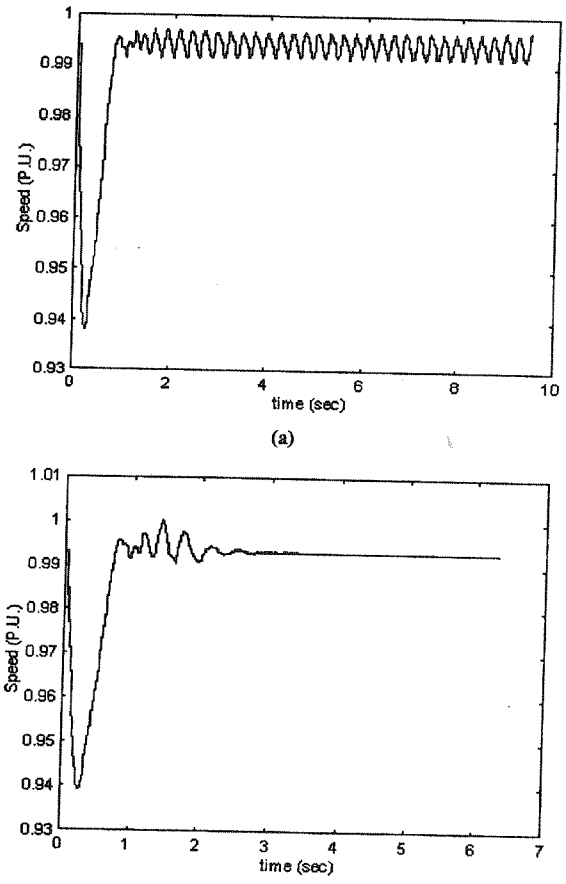

(a) :CSVC, (b): FLSVC

Fig. (19) Speed variations of the equivalent double cage machine during fault analysis test.

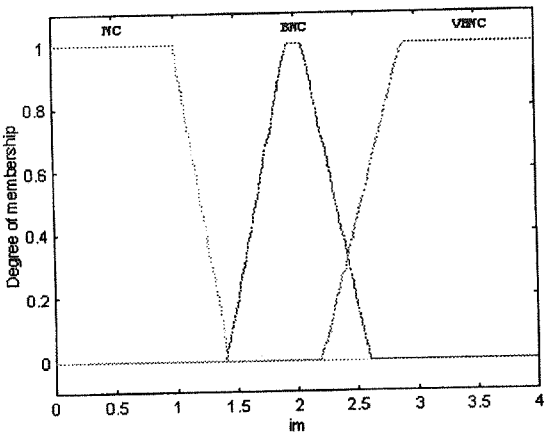

Fig. (10) Normalized symmetrical trapezoidal membership function for the first input (Ism p. u.) in the proposed FLSSE

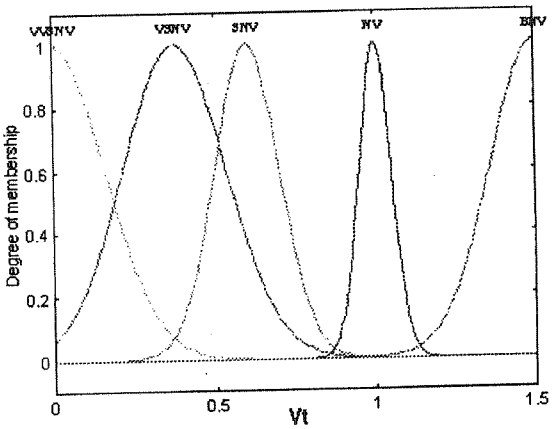

Fig. (11) Normalized symmetrical Gaussian membership function for the second input (Vt p. u.) in the proposed FLSSE

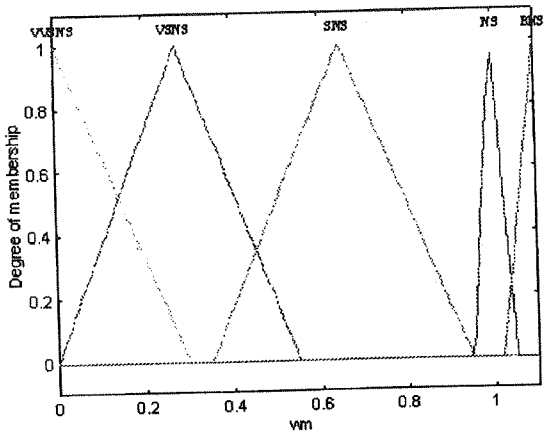

Fig. (12) Normalized symmetrical trapezoidal membership function for the output (ω_{rsm})

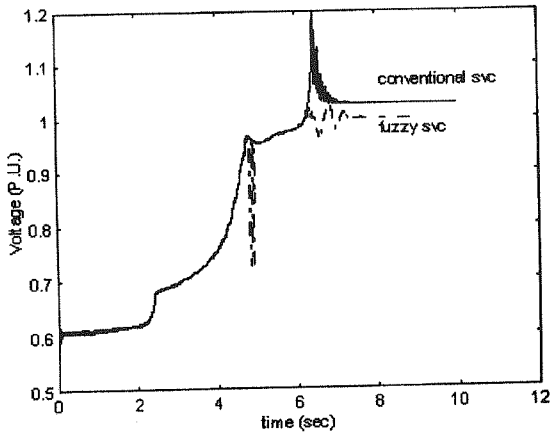

Fig. (13) Main terminal voltage (Vt) during the run-up test

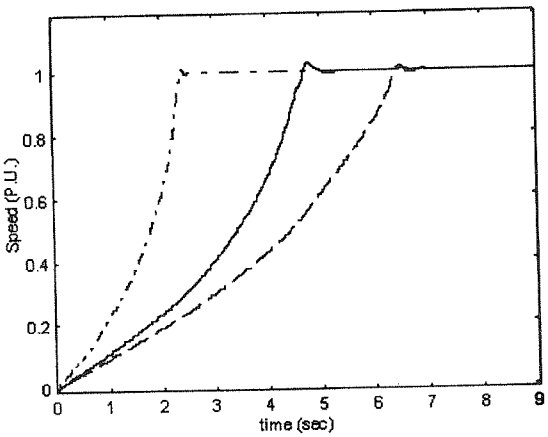

(a) : CSVC

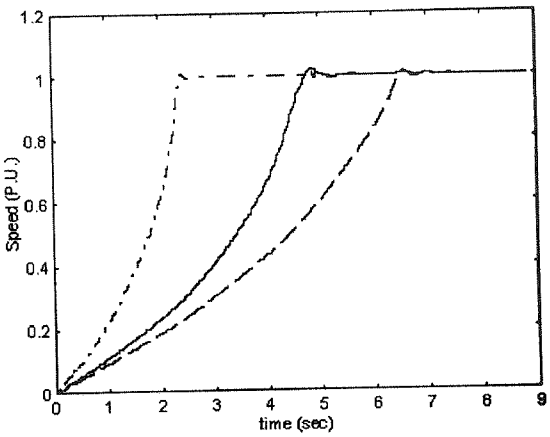

(b) : FL SVC

Fig. (14) Speed variations for all electric motors during the run-up test.

Table (3): Parameters of the transmission lines

	L1	L2
R (pu)	0.01	0.01
X (pu)	0.0314	0.0314

Table (4) Parameters for each asynchronous motor.

	SCAM	DCAM
Rs (pu)	2.476	0.117
Rr (pu)	1.767	-
Rr1 (pu)	-	0.174
Rr2 (pu)	-	3.259
Xlr1 (pu)	-	2.695
Xlr2 (pu)	-	1.98
Xlr (pu)	11.399	-
Xm (pu)	510.58	86.576
Trot (pu)	0.0003	0.0001
H (s)	0.0022	0.082
Rated Power (hp)	500	4700
Rated voltage (V)	2300	2300

Table (5) Parameters for each synchronous motor.

	SM
Rs (pu)	0.0121
Rfd (pu)	0.00145
Rkd (pu)	0.0302
Rkq1 (pu)	0.039
Xkq2 (pu)	10
Xs (pu)	0.14
Xlfd (pu)	0.267
Xlkd (pu)	0.092
Xlkq1 (pu)	0.115
Xlkq2 (pu)	10
Xmq (pu)	0.75
Xmd (pu)	1.03
Trot (pu)	0.0001
H (s)	1
Rated Power (hp)	6000
Rated voltage (V)	2300

Table (6) Parameters for both FLSVC, and CSVC schemes.

	FLSVC	CSVC
Tv (s)	0.	0.
Ta (s)	0.05	0.05
Ka	40	40
Ti (s)	-	0.08
Ki	-	0.0105
Bc (pu)	11	11
Bf max (pu)	12	12

$$[A_{11}] = \text{diag}[\ X_m + X_{LS} \qquad X_m + X_{LS}\ ]$$

$$[A_{12}] = [A_{21}] = \text{diag}[\ X_m \quad X_m]$$

$$[A_{22}] = \text{diag}[\ X_m + X_{Lr} \qquad X_m + X_{Lr}\ ]$$

$$[B_{11}] = \begin{bmatrix} R_s & \frac{\omega_{rsm}}{\omega_b}(X_{LS} + X_m) \\ -\frac{\omega_{rsm}}{\omega_b}(X_{LS} + X_m) & R_s \end{bmatrix}$$

$$[B_{21}] = \begin{bmatrix} 0 & \frac{\omega_{rsm} - \omega_{rsc}}{\omega_b} X_m \\ \frac{\omega_{rsc} - \omega_{rsm}}{\omega_b} X_m & 0 \end{bmatrix}$$

$$[B_{22}] = \begin{bmatrix} R_r & \frac{\omega_{rsm} - \omega_{rsc}}{\omega_b}(X_m + X_{Lr}) \\ \frac{\omega_{rsc} - \omega_{rsm}}{\omega_b}(X_m + X_{Lr}) & R_r \end{bmatrix}$$

For the double cage asynchronous motor we have:

$$[A] = \frac{1}{\omega_b}\begin{bmatrix} A_{11} & A_{12} & A_{13} \\ A_{21} & A_{22} & A_{23} \\ A_{31} & A_{32} & A_{33} \end{bmatrix}$$

$$[B] = -\begin{bmatrix} B_{11} & B_{12} & B_{13} \\ B_{21} & B_{22} & B_{23} \\ B_{31} & B_{32} & B_{33} \end{bmatrix}$$

and,

$$[A_{11}] = \text{diag}[\ X_{LS} + X_m \qquad X_{LS} + X_m\ ]$$

$$[A_{21}] = [A_{31}] = [A_{12}] = [A_{13}] = [A_{32}] = [A_{23}] =$$

$$\text{diag}[X_m \quad X_m]$$

$$[A_{22}] = \text{diag}[\ X_{Lr1} + X_m \qquad X_{Lr1} + X_m\ ]$$

$$[A_{33}] = \text{diag}[\ X_{Lr2} + X_m \qquad X_{Lr2} + X_m\ ]$$

$$[B_{11}] = \begin{bmatrix} R_s & \frac{\omega_{rsm}}{\omega_b}(X_{LS} + X_m) \\ -\frac{\omega_{rsm}}{\omega_b}(X_{LS} + X_m) & R_s \end{bmatrix}$$

$$[B_{12}] = [B_{13}] = \begin{bmatrix} 0 & \frac{\omega_{rsm}}{\omega_b} X_m \\ -\frac{\omega_{rsm}}{\omega_b} X_m & 0 \end{bmatrix}$$

$$[B_{21}] = [B_{23}] = [B_{31}] = [B_{32}]$$

$$[B_{21}] = \begin{bmatrix} 0 & \frac{\omega_{rsm} - \omega_{rdc}}{\omega_b} X_m \\ \frac{\omega_{rdc} - \omega_{rsm}}{\omega_b} X_m & 0 \end{bmatrix}$$

$$[B_{22}] = \begin{bmatrix} R_{r1} & \frac{\omega_{rsm} - \omega_{rdc}}{\omega_b} X_{r1} \\ \frac{\omega_{rdc} - \omega_{rsm}}{\omega_b} X_{r1} & R_{r1} \end{bmatrix}$$

$$[B_{33}] = \begin{bmatrix} R_{r2} & \frac{\omega_{rsm} - \omega_{rdc}}{\omega_b} X_{r2} \\ \frac{\omega_{rdc} - \omega_{rsm}}{\omega_b} X_{r2} & R_{r2} \end{bmatrix}$$

but,

$$X_{r1} = X_{Lr1} + X_m \ , \ X_{r2} = X_{Lr2} + X_m$$

Appendix 2

This appendix provides the necessary data for the studied sample system.

$\omega_s = \omega_b = 377$ rad/s

$S_{base} = 100$ MVA

All transformers are assumed to be ideal (R = X = 0). External network is also considered to be an ideal voltage source (Rg = Xg = Bg = 0).

quadrature axis of the synchronous machine respectively.

Kd, fd :damper and field winding quantities along direct axis of the synchronous machine respectively

md, mq: mutual quantities along direct and quadradure axis of the synchronous motor respectively

c, f: fixed capacitor and variable reactor quantities in SVCs

TCR: thyristor controlled reactor

SVC: terminal busbar in SVC schemes

t: main terminal busbar

g: external network

Greek letters

δ_{rsm}: rotor angle of the synchronous motor

ω_{rsm}: rotor speed of the synchronous machine

ω_s: synchronous speed

ω_b: radian frequency base

ω_{rsc} , ω_{rdc} : rotor speed of the single and double cage asynchronous motors respectively

Appendix 1

In this appendix the elements of [A], and [B] matrices for synchronous and asynchronous motors are given . For the sysnchronous motor we have:

$$[A]=\frac{1}{\omega_b}\begin{bmatrix} A_{11} & A_{12} & A_{13} \\ A_{21} & A_{22} & 0 \\ A_{31} & 0 & A_{33} \end{bmatrix}$$

$$[B]=-\begin{bmatrix} B_{11} & B_{12} & B_{13} \\ 0 & B_{22} & 0 \\ 0 & 0 & B_{33} \end{bmatrix}$$

and,

$$[A_{11}]=\mathrm{diag}\begin{bmatrix} X_d & X_q \end{bmatrix}$$

$$[A_{12}]=[A_{21}]^t=\begin{bmatrix} X_{mq} & X_{mq} \\ 0 & 0 \end{bmatrix}$$

$$[A_{13}]=[A_{31}]^t=\begin{bmatrix} 0 & 0 \\ X_{md} & X_{md} \end{bmatrix}$$

$$[A_{22}]=\begin{bmatrix} X_{kq1} & X_{mq} \\ X_{mq} & X_{kq2} \end{bmatrix}$$

$$[A_{33}]=\begin{bmatrix} X_{fd} & X_{md} \\ X_{md} & X_{kd} \end{bmatrix}$$

$$[B_{11}]=\begin{bmatrix} R_s & \omega_{rsm}\frac{X_d}{\omega_b} \\ -\omega_{rsm}\frac{X_q}{\omega_b} & R_s \end{bmatrix}$$

$$[B_{12}]=\begin{bmatrix} 0 & 0 \\ -\omega_{rsm}\frac{X_{mq}}{\omega_b} & -\omega_{rsm}\frac{X_{mq}}{\omega_b} \end{bmatrix}$$

$$[B_{22}]=\mathrm{diag}\begin{bmatrix} R_{kq1} & R_{kq2} \end{bmatrix}$$

$$[B_{33}]=\mathrm{diag}\begin{bmatrix} X_{md} & R_{kd} \end{bmatrix}$$

$$[B_{13}]=\begin{bmatrix} -\omega_{rsm}\frac{X_{md}}{\omega_b} & -\omega_{rsm}\frac{X_{md}}{\omega_b} \\ 0 & 0 \end{bmatrix}$$

For the single cage asynchronous motor we have:

$$[A]=\frac{1}{\omega_b}\begin{bmatrix} A_{11} & A_{12} \\ A_{21} & A_{22} \end{bmatrix}$$

$$[B]=-\begin{bmatrix} B_{11} & B_{12} \\ B_{21} & B_{22} \end{bmatrix}$$

and,

to 1pu. However the CSVC provides 10 percent overvoltage.

Fig. 22 depicts the rotor angle variations of the equivalent sysnchronous motor. It is clear that the CSVC is not able to save the synchronous motor (i.e., transient unstable). Fig. 23 illustrates the speed variations of the equivalent double cage asynchronous motor in this test. It is obvious that the CSVC scheme causes the instability for double cage machine, and pulsating vibrations would be appeared on the motor shaft.

6 - Conclusions

This paper presents a novel fuzzy logic based static VAR compensator (FLSVC), applied to an industrial power system. The following issues have been addressed:

1 - complete representation of non-linear characteristics of the given power network.

2 - appropriate selection of membership functions and rule set based on the control system objectives.

3 - verification of the proposed sensorless fuzzy logic controller capabilities, by non - linear time domain digital simulations under various operating conditions and disturbances.

The main achievements are:

a - the proposed FLSC, improves the voltage profile and overall dynamic and transient performance for the given plant, compared to the conventional SVC.

b - the non - linear characteristics of the system as well as different operating points can be easily incorporated into the controller development by suitable selection of membership functions and rule set.

c - the proposed sensorless FLC, which has remarkable effects on the transients and dynamic performance of the given plant has been established by considering only two inputs ($\Delta\omega_{rsm}$, and $\Delta\dot{\omega}_{rsm}$). and one output (Us). The inputs have been estimated by novel fuzzy logic based speed sensorless scheme (FLSSE), and accompanied differentiator like function (DLF), block. This controller represents a simple nonlinear adaptive controller.

d - the proposed FLSVC, is simple to develop and easy to implement.

e - with some slight modifications, the proposed FLSVC, can be easily applied, especially, to flexible AC transmission systems (FACTS).

7 - Nomenclature

R, X: resistance and reactance

v , i: voltage ad current

B: susceptance

Te, T_L: electromagnetic and load torques

Trot: rotational torque

H: inertia constant

[ ]^t : matrix transpose

p: derivative operator d/dt

t: time (s)

Subscripts

s: stator quantities for all electric motors

r : rotor quantities of the single cage asynchronous motor

r1, r2: upper and lower cage quantities in the double cage machine

d. q: direct and quandrature axes quantities respectively

L: leakage

m: magnetizing quantities for asynchronous motor

kq1, kq2: damper winding quantities along

t = 0. The ESM is treated as asynchronous motor during starting period, and the field voltage is applied when the rotor speed has been reached to 90 percent of synchronous speed. It is further assumed that the equivalent static load (ESL) is also connected to its supply transformer at t=0. Fig. 13 shows the voltage profile of the main terminal busbar (v_t), during the run - up test for both FLSVC, and CSVC schemes. It is clear that the voltage drops to 0 .6 pu immediately after simultaneous starting. As observed, the FLSVC remarkably settles the voltage to 1pu, but the CSVC eventually provides 3 percent over voltage due to its current feedback path.

Fig. 14 depicts the speed variations of all equivalent motors. It can be seen that for both schemes, the speed variations of all motors are roughly similar.

Case 2: Sudden loading test

Suppose that all no load motors are completely started, and a sudden loading test is then perfomed at t =0 . The load torque for each motor assumed to be 1pu (T_L = 1pu), based on its own rating. Figs. 15 shows the main terminal voltage (v_t) due to the performance of both schemes. For this case, we also observe that the porposed FLSVC, works well and settles the voltage to 1pu, however the CSVC eventually provides 5 percent over voltage due to its current feedback loop.

Fig. 16 depicts the speed variations of both equivalent single and double cage asynchronous motor. Fig. 17 illustrates the rotor angle variations of equivalent synchronous motor.

Case 3: Fault analysis

In this case the effects of voltage dips caused by three phase fault within the industrial network will be evaluated. Suppose that the sudden loading test is completely accomplished, and the whole system components are operating in the steady state conditions. Let the three phase fault to be occurred at point F shown in Fig. 1, at t = 0 and cleared at t = 133 ms (i.e., circuit breakers labelled by B2 and B4 are opened after 8 cycles). Fig. 18 shows the main terminal busbar voltage (v_t) during the fault analysis test . It worths to observed the high performance of the FLSVC, for this case too. As easily seen in Fig. 18, the main terminal busbar (v_t), settles to lpu, whereas the CSVC cause voltage fluctuations (i. e., voltage instability).

Fig. 19 depicts the speed variations of equivalent double cage asynchronous motor. It can be seen that this motor becomes unstable due to functionality of CSVC scheme (i. e. pulsating vibrations would be appeared on the motor shaft). Fig, 20 shows the rotor angle variations of the equivalent synchronous motor . It is clear that the CSVC scheme is not able to avoid instability.

Case 4: Voltage dips analysis

In this case the effects of voltage dips in the remote external network will be evaluated. Suppose that the whole system components are operating in the steady state conditions. Let the momentary voltage dips to be occurred in the remote external network at t = 0 (Eg = 0. 4 pu), and recovered to its nominal value (E_g=1pu) after 20 cycles. Fig. 21 shows voltage variations at the main terminal busbar (v_t). Obviously one can see that the FLSVC settles the voltage

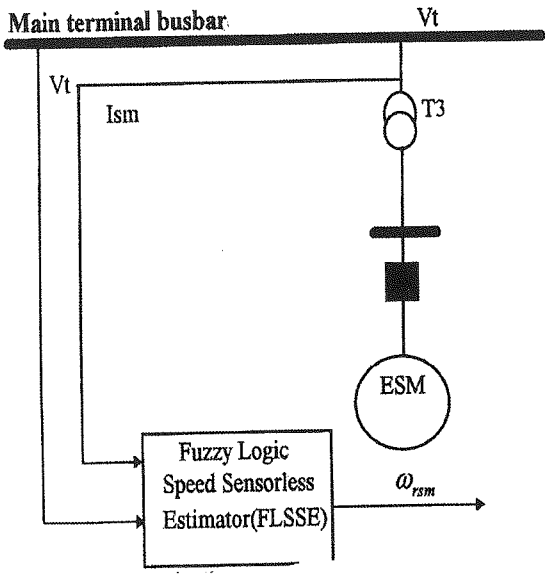

Fig .(9) Schematic diagram of the fuzzy logic based speed sensorless estimator (FLSSE)

B - Fuzzy logic based speed sensorless estimator (FLSSE)

The basic configuration of the FLSSE used in the proposed FLSVC is shown in Fig. 9. The building blocks of FLSSE is similar to those shown in Fig. 4.

However, the inputs of the proposed FLSSE are the total current (Ism) of all synchronous motors (ESM), and the voltage of the main terminal busbar (V_t). This voltage is readily available in FLSVC scheme (i. e. the input of H (s) in Fig. 3). The current (Ism) could be also detected closely to the FLSVC scheme. For present investigation three trapezoidal membership functions are considered for the first input variable (i.e. current). For the second input variable (i.e. voltage of the main terminal busbar), five Gaussian membership functions are sufficient . For the output fuzzy variable (i.e. estimated speed, ω_{rsm}), five triangular membership functions are assumed. Figs. 10 to 12 depict the membership functions for input and output fuzzy variables for the proposed FLSSE.

A fuzzy rule set is then used to describe the FLSSE behaviour as shown in Table. 2. Each entry of this table also represents a rule of the form" if accident then consequences". The entities of this table could be derived easily due to expert knowledge and deep investigation into physical aspects of synchronous motors , and dependency of speed variations respect to terminal voltage and current.

The appropriate crisp output singnal (i.e. estimated speed, $\Delta\omega_{rsm}$ could be generated by correlation product inference and center of gravity defuzzification method [30, 31]. In this study due to complete similarities of all synchronous motors in the given plant, the estimated speed of each synchronous motor is also similar to the output of the proposed FLSSE.

5 - Simulation studies

In this section various comparative digital simulation tests are demonstrated for the sample system given in Fig. 1. To show the capabilities and effectiveness of the proposed FLSVC, the results are compared with the performance of the CSVC. The simulations are performed in the well established computing environment called MATLAB accompanied with its FUZZY LOGIC TOOLBOX. In the following cases the value of voltage source in the remote external network (Eg), is set to 1pu, unless stated. The system data are given in the appendix 2.

Case 1: Run-up test

In this case it is assumed that the no load ESCAM, EDCAM, and ESM are started at

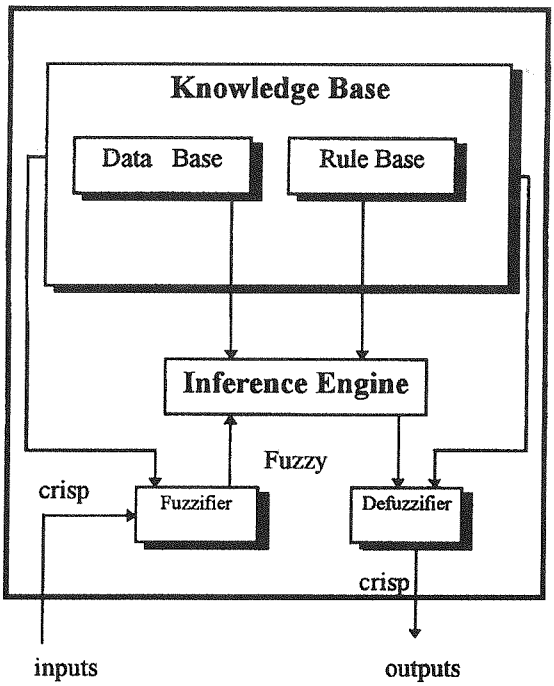

Fig. (4) Schematic diagram of the FLC building blocks.

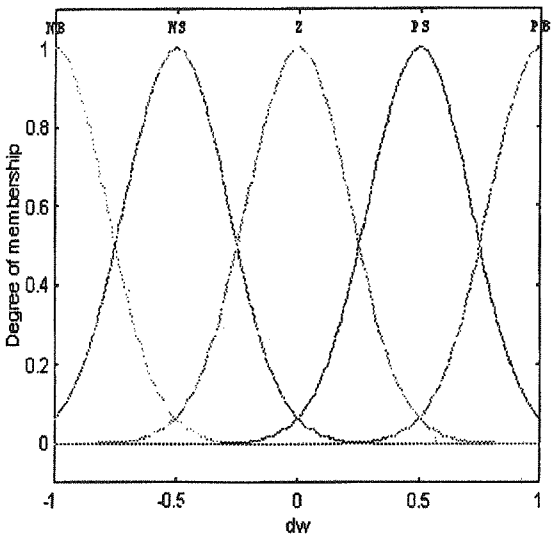

Fig. (5) Normalized symmetrical Gaussian membership function for the first input (Dwrsm) in the proposed FLC

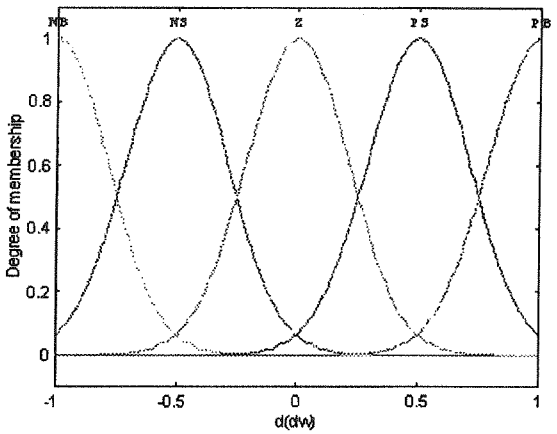

Fig. (6) Normalized symmetrical Gaussian membership function for the second input (Dwrsm) in the proposed FLC

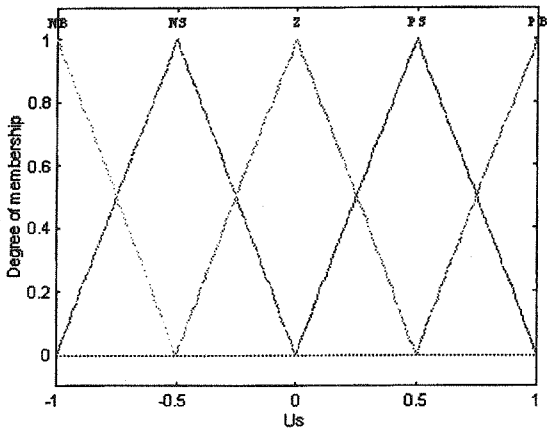

Fig. (7) Normalized symmetrical triangular membership function for the output (Us) in the proposed FLC

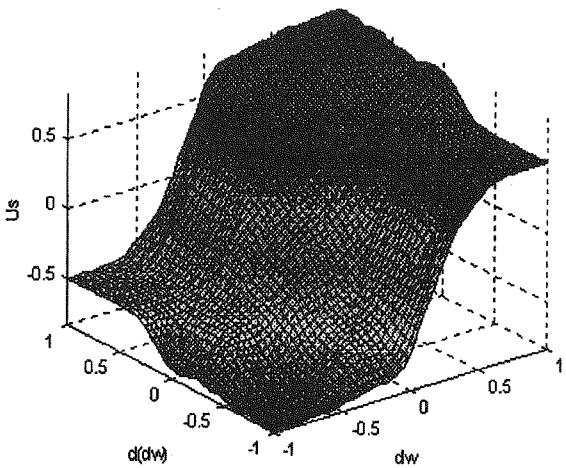

Fig. (8) Three dimensional plot of interrelations between the FLC inputs and output.

priate crisp control signal is then generated [30, 31]. Fig 8 shows the three dimensional view of the interrelation between the crisp values of output signal, an FLC inputs, which graphically represents the nonlinear performance of the proposed FLC.

Table 1. A sample set of 5 x 5 rules for proposed FLC

$\Delta\dot{\omega}_{rsm}$ / $\Delta\omega_{rsm}$	NB	NS	Z	PS	PB
NB	NB	NB	NB	NS	NS
NS	NB	NB	NS	NS	NS
Z	NB	NS	Z	PS	PB
PS	PS	PS	PS	PB	PB
PB	PS	PS	PB	PB	PB

NB: negative big, NS: negative small
Z: Zero, PB: positive big, PS: positive small

Table 2. A sample set of 5 x 3 rules for the proposed FLSSE

Ism / Vt	NS	BNC	VBNC
VVSNV	NH	VVSNV	VVSNS
VSNV	NH	VSNS	VSNS
SNV	NH	SNS	SNS
NV	NS	NH	NH
BNV	BNS	NH	NH

NC: Normal Current, BNC: Bigger than Normal Current, VBNC: Very Bigger than Normal Current, NV: Normal Voltage SNV: Smaller than Normal Voltage, VSNV: Very Smaller than Normal Voltage, VVSNV: Very Very Smaller than Normal Voltage, NS: Normal speed , BNS: Bigger than Normal Speed, SNS: Smaller than Normal Speed, VSNS: Very Smaller than Normal speed NH: Never Happens

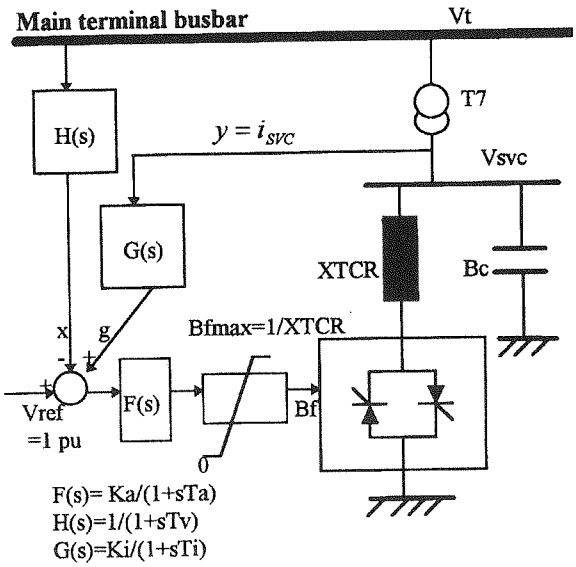

Fig. (2) Conventional SVC.

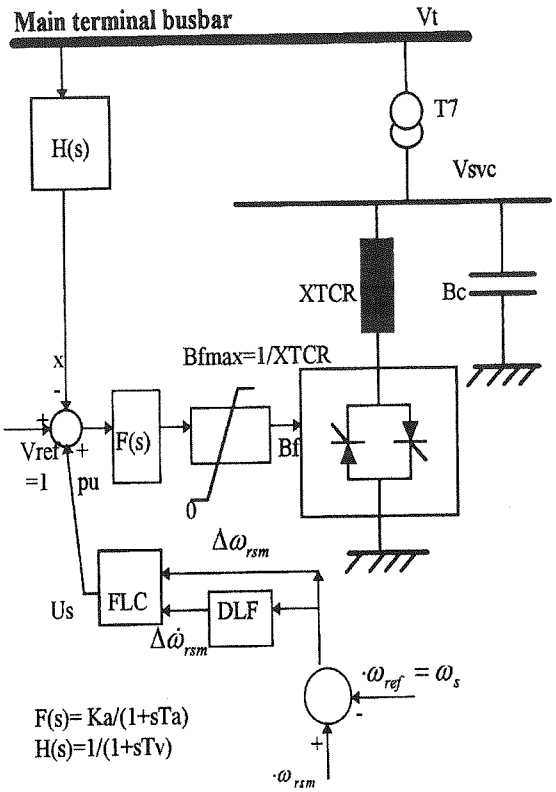

Fig. (3) Schematic diagram of the FLSVC.

($\Delta\omega_{rsm}$), and the associated acceleration ($\Delta\dot{\omega}_{rsm}$), of the equivalent synchronous motor (ESM) are chosen as the FLC inputs. Note that,

$$\Delta\omega_{rsm} = \omega_s - \omega_{rsm} \qquad (20)$$

ω_{rsm} can be easily detected by conventional mechanical sensor and/or estimated by speed sensorless schemes. In the conventional speed detecting scheme (i. e, use of mechanical sensor), due to complete similarities of all SMs in the given plant, $\Delta\omega_{rsm}$ and $\Delta\dot{\omega}_{rsm}$ of each SM would be similar to those of the ESM. Hence in practice $\Delta\omega_{rsm}$ and $\Delta\dot{\omega}_{rsm}$ related to one of these SMs should be used as the FLC inputs.

In this paper a novel fuzzy logic based speed sensorless estimator (FLSSE) is presented to predict the actual speed of specific synchronous motor (ω_{rsm}). The proposed FLSSE, is fully described in part B of this section. Therefore $\Delta\omega_{rsm}$ can be readily obtained. $\Delta\dot{\omega}_{rsm}$ signal stems from $\Delta\omega_{rsm}$ and the additional differentiator like function (DLF), block shown in Fig. 3. The functionality of the DLF block could be easily determined by mathematical expression given in Eq. 21.

$$\Delta\dot{\omega}^{K+1}_{rsm} = \frac{\Delta\omega^{K+1}_{rsm} - \Delta\omega^{K}_{rsm}}{t^{K+1} - t^{K}} \qquad (21)$$

Thus two input signals of the proposed FLC become available. The output control signal (Us) is then injected to the summing point shown in Fig. 3.

Each pair of the FLC input and output fuzzy variables (Xj = $\Delta\omega_{rsm}$, $\Delta\dot{\omega}_{rsm}$, Us) is interpreted into the five linguistic fuzzy subsets varying from, Negative Big (NB) to Positive Big (PB). Figs 5 and 6, respectively illustrate normalized symmetrical Gaussian membership functions related to $\Delta\omega_{rsm}$ and $\Delta\dot{\omega}_{rsm}$. The choice of these five membership functions for each input fuzzy variable is based on the simulation studies of the sample system shown in Fig. 1, without functionality of any SVC scheme. The range of variations of the desired input variables ($\Delta\omega_{rsm}$ and $\Delta\dot{\omega}_{rsm}$), for the given plant without any voltage regulating device, helped us to judge that the five membership functions are reasonably suitable for input variables.

It is also understood that the five normalized symmetrical triangular membership functions given in Fig. 7, are appropriate for the controller output (Us), in order to have more reasonable results and an easy real time implementation. The input gains (k 1, and k2), and the output gain (k3), are normally used to properly scale the fuzzy input and output variables, respectively. In the present study we set these parameters as follows:

$$k1 = 1 \ , k2 = 10 \ , k3 = 12$$

A fuzzy rule set is then used to describe the FLC behaviour as shown in Table 1. Each entry in this table represents a rule of the form "if accident then consequence", e.g.

if ($\Delta\omega_{rsm}$) is NS and ($\Delta\omega_{rsm}$) is NB then Us is NB.

The entities of Table 1, could be derived due to expert knowledge. Here, these rules are obtained through a deep investigation into physical aspects of the sample system and the digital simulation results belonging to the given industrial plant without consideration of any SVC scheme. Using the correlation product inference and center of gravity defuzzification method, the appro-

feedback path (G(s)) is vanished. The firing angle regulator (F(s)) and its limiter block appeared in the forward path of both SVC schemes are suitable for transient and dynamic studies and is widely used in industry [28-29]. The proposed FLC development will be fully described in the next section.

For the simulation purposes, dq models based on the rotating frame of reference are required for the fixed capacitor and variable reactor in both schemes. Ignoring the transient terms, the ideal lossless thyristor controlled reactor can be represented as [11]:

$$\begin{bmatrix} v_{qTCR} \\ v_{dTCR} \end{bmatrix} = \begin{bmatrix} 0 & \frac{\omega_{rsm}}{\omega_b} X_{TCR} \\ -\frac{\omega_{rsm}}{\omega_b} X_{TCR} & 0 \end{bmatrix} \begin{bmatrix} i_{qTCR} \\ i_{dTCR} \end{bmatrix} \quad (13)$$

where,

$$X_{TCR} = \frac{1}{B_f}$$

with the same argument the fixed capacitor can also be represented as:

$$\begin{bmatrix} v_{qSVC} \\ v_{dSVC} \end{bmatrix} = \begin{bmatrix} 0 & -\frac{\omega_{rsm}}{\omega_b} X_c \\ \frac{\omega_{rsm}}{\omega_b} X_c & 0 \end{bmatrix} \begin{bmatrix} i_{qc} \\ i_{dc} \end{bmatrix}$$

where,

$$X_C = \frac{1}{B_C}$$

Eq. 14, can also be applied for the shunt susceptance (Bg) modeling in the remote external network. The state space equations concerning the state variables in Fig. 2, suitable for digital simulations are:

$$T_v \dot{\chi} + \chi - v_t = 0 \quad (15)$$

$$T_a \dot{\beta}_f + B_f - K_a (V_{ref} - \chi + g) = 0 \quad (16)$$

$$T_i \dot{g} + g - K_i y = 0 \quad (17)$$

The following state space equations dealing with the state variables in Fig. 3, are also used for comparative digital simulations:

$$T_v \dot{\chi} + \chi - v_t = 0 \quad (18)$$

$$T_{a\alpha} \dot{\beta}_f + B_f - K_a (V_{ref} - \chi + U_s) = 0 \quad (19)$$

In both schemes we have:

$$0 \le \dot{B}_f \le \frac{1}{X_{TCR}}$$

and:

$$v_t = (v^2_{td} + v^2_{tq})^{1/2}$$

4 - Fuzzy logic-based static VAR compensator (FLSVC)

A: Control structure

The basic configuration of the FLC used in the proposed FLSVC shown in Fig. 4 is simply represented by four main parts: the fuzzifier, the knowledge base, The inference engine and the defuzzifier. The fuzzifier maps the FLC input crisp values scaled by input gains into fuzzy variables using normalized membership functions. The fuzzy logic inference engine then infers the proper control actions based on the given fuzzy rule base. The fuzzy control action is in turn translated into the proper crisp values scaled by some appropriate output gains through the defuzzifier employing normalized membership functions [30].

The feature of constant speed operation makes it even more complex for synchronous motors (SMs) to obtain operation continuity in the presence of voltage disturbances, therefore the speed deviation

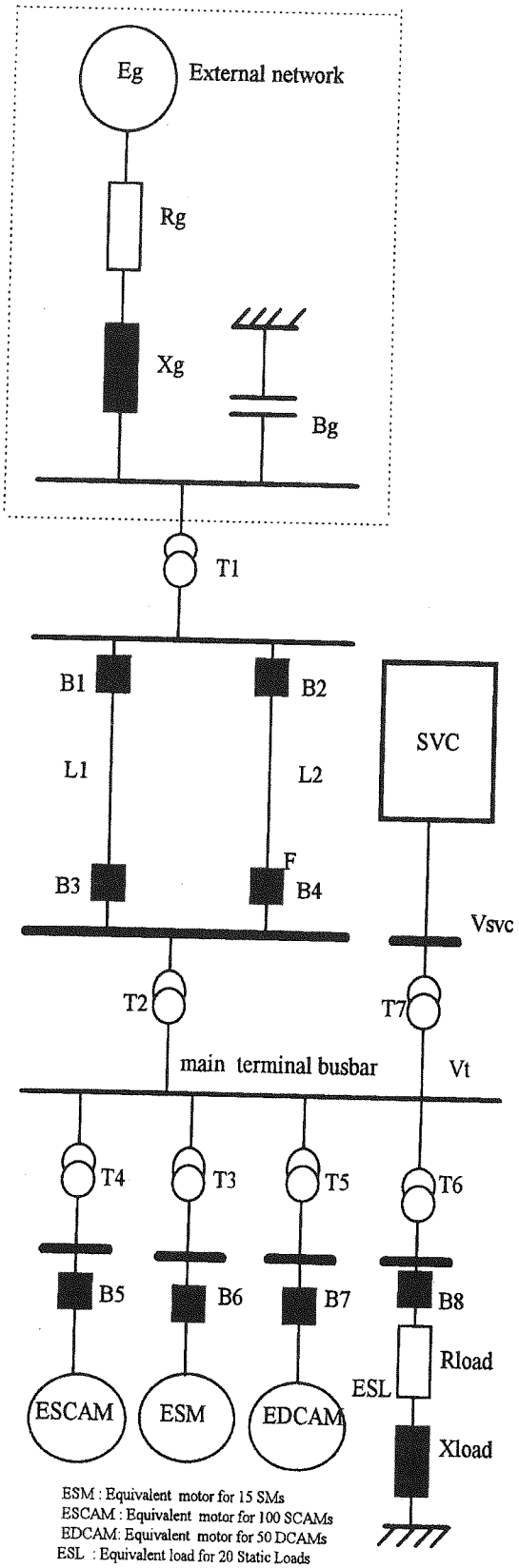

Fig. (1) The sample system single line diagram

where,

$$[C]=\begin{bmatrix} \frac{-R_{se}\,\omega_b}{X_{se}} & -\omega_{rsm} \\ \omega_{rsm} & \frac{-R_{se}\,\omega_b}{X_{se}} \end{bmatrix}$$

$$\begin{bmatrix} v_{qse} \\ v_{dse} \end{bmatrix}=\begin{bmatrix} v_{qi} \\ v_{di} \end{bmatrix}-\begin{bmatrix} v_{qk} \\ v_{dk} \end{bmatrix} \qquad (12)$$

In Eq. 12, the indices i, and k, respectively, denote the terminal busbars of each series element. Eq. 11, is also suitable to represent a series impedance of the external network (Rg, Xg). For equivalent static load (ESL) modeling, we may still apply Eq. 11, with the following modifications:

$$v_{qk} = v_{dk} = 0\ ,\ R_{se} = R_{load}\ ,\ X_{se} = X_{load}$$

3-4: The SVC model

The SVC shown in Fig. 1 is a three phase thyristor controlled reactor/fixed capacitor type (TCR/FC) . In this paper two distinct control strategies have been employed for comparative digital simulations. The first scheme, which is commonly refered to conventional SVC (CSVC), is shown in Fig. 2 [10. 11]. The CSVC includes voltage and current feedback paths (i.e, H (s) and G (s)), firing angle regulator (F (s)), and the associated limiter block as well.

In the second scheme shown in Fig. 3 the proposed FLC, represents a two inputs-single output non-linear controller. Both speed deviation ($\Delta\omega_{rsm}$), and associated acceleration ($\Delta\dot{\omega}_{rsm}$) of equivalent synchronous motor are taken as the inputs. In recent fuzzy logic based SVC (FLSVC), voltage feedback path (H(s)), firing angle regulator (F (s)), and limiter block are similar compared to the conventional one, while the current

$$p\left(\frac{\omega_{rsm}}{\omega_b}\right)=\frac{1}{2H}\left(T_e - T_L - T_{rot}\right) \quad (2)$$

and,

$$p\left(\frac{\delta_{rsm}}{\omega_b}\right)=\frac{\omega_{rsm}}{\omega_b} - 1 \quad (3)$$

where,

$$T_e = X_{md} I_d i_{qs} - X_{mq} I_q i_{ds} \quad (4)$$

and,

$$I_d = i_{ds} + i_{fd} + i_{kd} \;,\; I_q = i_{qs} + i_{kq1} + i_{kq2}$$

3-2- Three phase asynchronous motor modeling

Three phase equivalent single cage asynchronous motor (ESCAM) which is also shown in Fig. 1, is represented by a fifth order model in the rotating dq frame of reference environment [27] with the followig dynamic equation.

$$p[i]=[A]^{-1}[[B][i]+[V]] \quad (5)$$

where

$$[i]=[i_{qs} \quad i_{ds} \quad i_{qr} \quad i_{dr}]^t$$

$$[V]=[v_{qs} \quad v_{ds} \quad 0 \quad 0]^t$$

The motion equation for the ESCAM is [27]:

$$p\left(\frac{\omega_{rsc}}{\omega_b}\right)=\frac{1}{2H}\left(T_e - T_L - T_{rot}\right) \quad (6)$$

where

$$T_e = X_m (i_{qs}\, i_{dr} - i_{ds}\, i_{qr}) \quad (7)$$

An equivalent three phase double cage asynchronous motor (EDCAM) is represented by a seventh order model in the rotating dq axes environment [27] as:

$$p[i]=[A]^{-1}[[B][i]+[V]] \quad (8)$$

where,

$$[i]=[i_{qs} \quad i_{ds} \quad i_{qr1} \quad i_{dr1} \quad i_{qr2} \quad i_{dr2}]^t$$

$$[V]=[v_{qs} \quad v_{ds} \quad 0 \quad 0 \quad 0 \quad 0]^t$$

The mechanical dynamic equation for the EDCAM is [27]:

$$p=\left(\frac{\omega_{rdc}}{\omega_b}\right)=\frac{1}{2H}\left(T_e - T_L - T_{rot}\right) \quad (9)$$

where,

$$T_e = X_m[i_{qs} \quad I_{dr12} - \quad i_{ds} \quad I_{qr12}] \quad (10)$$

and,

$$I_{dr12} = i_{dr1} + i_{dr2}$$

$$I_{qr12} = i_{qr1} + i_{qr2}$$

The elements of [A] and [B] for both asynchronous motors are given in appendix 1.

3-3- Transmission line, transformer and static load modeling

Each transmission line and/or transformer, given in Fig. 1 is represented by a series resistance and reactance, Rse, Xse respectively . The dq model based on the rotating frame of reference for each series element is [11]:

$$p\begin{bmatrix} i_{qse} \\ i_{dse} \end{bmatrix}=\frac{\omega_b}{X_{se}}\begin{bmatrix} v_{qse} \\ v_{dse} \end{bmatrix}+[C]\begin{bmatrix} i_{qse} \\ i_{dse} \end{bmatrix} \quad (11)$$

(FLSSE), is employed which is one of the main distinct features of present study. The advantages of proposed FLSSE are lower cost, elimination of cables belonging to mechanical speed sensor of a remote specific machine, and increased reliability.

The performance of the proposed FLSVC is examined by several non - linear time - domain simulation tests. These tests have been performed in different operating conditions and disturbances, such as motor starting and loading, and momentary voltage dips. The results show that the FLSVC, remrkably improves the voltage profile and the overall system performance compared to those of the system which is equipped with a conventional SVC (CSVC).

2 - System description

Fig. 1 shows the single line diagram of three phase studied industrial power system. To feed the main terminal busbar of the load center, the remote external network is connected to a step - up transformer (T1), a double circuit transmission line (L1, L2), and a step-down transformer (T2). In the present study the plant consists of hundred similar SCAMs, fifty unique rating DCAMs, and fifteen similar SMs. In present study, the load torque and duty cycles are assumed to be similar for all synchronous motors. Therefore they can justifiably considered to be coherent [26]. So they may be represented by an equivalent synchronous motor (ESM), fed by a step - down transformer (T3). The same argument can be implemented for a group of similar single and double cage asynchronous motors. Thus two equivalent machines (ESCAM, EDCAM) shown in Fig. 1 are sufficient for the present study.

It is further assumed that the plant also includes twenty static loads, which is considered to act as an equivalent three phase static load (SL) supplied by an additional transformer (T6). The SVC, which is connected to the main terminal busbar via an auxiliary transformer (T7), is a three phase thyristor controlled reactor/fixed capacitor type (TCR/FC).

3 - System modeling

This section presents different distinct models for the system components given in Fig. 1, which are appropriate for digital simulations. The models are mostly based on the rotating dq frame of reference. For synchronous motor representation it is assumed that dq axes are fixed to the rotor winding (i.e, Park's model). To avoid frame transformation it is further assumed that the arbitrary speed of rotating dq axes assigned to other components is equal to the speed of equivalent synchronous motor (ω_{rsm}).

3-1- Three phase synchronous motor modeling

The three phase equivalent synchronous motor (ESM) shown in Fig. 1, is represented by Park's seventh order model [27]. Hence:

$$p[i] = [A]^{-1}[[B][i] + [V]] \qquad (1)$$

where

$$[i] = [i_{qs} \quad i_{ds} \quad i_{kq1} \quad i_{kq2} \quad i_{fd} \quad i_{kd}]^t$$

$$[V] = [v_{qs} \quad v_{ds} \quad 0 \quad 0 \quad v_{fd} \quad 0]^t$$

The elements of [A] and [B] are given in appendix 1. The motion equation for the ESM is [27]:

equipment voltage during and immediately after the momentary disturbance of supply voltage so that the satisfactory functioning of the equipment is preserved.

The operation continuity of the sensitive equipment composed of synchronous and asynchronous motor loads, subjected to unavoidable momentary voltage dips is of particular interest [7, 8]. Traditional practice such as reclosing and bus-transfer schemes have been applied for enhancing the operation continuity while it is necessary to consider preventive measures to minimize the risk of motor damage. The technique of riding through momentary voltage dips by keeping motors connected to their source during a voltage sag can minimize potential harmful effects to the motors and enhance operation reliability [8]. This technique can be further improved by voltage stabilization at the point of service by installing a SVC.

In large industrial installations, voltage drops due to motor starting may also occur for a certain interval of time. Various studies [9, 10] have proved that the SVCs can also be applied to start large three phase electrical motors, since they support the voltage and start-up torque and minimize the start-up time. These studies prove that fast controllable injection of reactive power by SVCs not only decreases the inrush start-up currents but also makes the reactive power demand to a certain minimum level during running conditions. Moreover, the continuous voltage support reduces the RI^2 losses. This is because of the decrease in motor reactive power demand with an increase in its terminal voltage [11].

Industrial power systems are highly nonlinear and stochastic in nature. So the controller parameters of specific regulating device can be optimum for one set of operating conditions but may not be suitable for another circumstances. Therefore, various investigators are studying how to use modern control techniques to improve the overall system performance.

As a well suited alternative to classical control strategies, the fuzzy logic based controller (FLC), has been suggested as an appropriate choice to control non-linear systems [12]. The basic feature of FLCs is that the control strategy can be simply expressed by a set of fuzzy rules which describe the behaviour of controller by employing linguistic terms. From these rules, the proper control action is then inferred. In addition FLCs are relatively easy to develop and simple to implement.

Some investigations have been performed in the area of applications of the FLCs in electric power systems [13-17]. However the implementation of the FLSVC within the synchronous and asynchronous motors plant has not been yet seen in the previous related studies [11, 18, 19, 20, 21]. The main objective of this paper is to enhance the voltage profile and the overall performance of an industrial utilization by using the FLSVC installed close to a synchronous and asynchronous motor load center.

For the current study, the FLC with two input signals are employed, while the output control signal is injected to SVC voltage regulator . The inputs of the proposed FLC are assumed to be speed and acceleration variations of a specific machine in the plant. To predict the speed signal, some speed sensorless schemes have been seen [22-25]. However in this paper the fuzzy logic based speed sensorless estimator

A Novel Sensorless Fuzzy Controller with Application to Static VAR Compensators in Industrial Power Systems

H. Rastegar
Assistant Professor

M. Abedi
Professor

M. B. Menhaj
Associate Professor

S. H. Fathi
Assistant Professor

Electrical Engineering Department
Amirkabir University of Technology

Abstract

The paper presents a simple yet powerful sensorless fuzzy logic based controller applied to static VAR compensator (SVC), in industrial power network consisting of three phase synchronous and asynchronous motor loads . In the proposed fuzzy logic based controller (FLC), the speed and acceleration variations of a specific machine are taken as the inputs. In this paper the supplementary fuzzy logic based speed sensorless estimator (FLSSE) is also employed to estimate the speed signal. To demonstrate the effectiveness and capabilities of the employed fuzzy logic based static VAR compensator (FLSVC), several non - linear time - domain digital simulation tests are performed. The results show that over a wide range of operating conditions and disturbances, the FLSVC improves remarkably the voltage profile and the overall dynamic performance of the plant compared to the conventional static VAR compensator (CSVC).

Keywords

Fuzzy Logic controller (FLC), Static VAR Compensator (SVC), Fuzzy Logic based Speed Sensorless Estimator (FLSSE), Single Cage Asynchronous Motor (SCAM), Double Cage Asynchronous Motor (DCAM), Synchronous Motor (SM).

1 - Introduction

Most voltage problems associated with sensitive equipments are related to momentary voltage dips which can occur due to faults in the supply system. The inability of sensitive equipment to function properly in the presence of momentary voltage sags raised a serious concern [1-3]. General measures to minimize the effects of momentary voltage dips, such system impedance, have major cost implications.

The effect of momentary voltage dips on the proper functioning of a particular sensitive equipment may be minimized by installing a fast - response voltage regulator at the point of service. This type of regulator includes static VAR compensator (SVC) [4-6] characterized by fast response time and virtually unlimited life as well. The general idea of applying a voltage regulator (i.e, SVC), is to optimally stabilize the